Scientific
Research
Publishing

Effect of Substitution Degree and the Calcination Temperature on the N₂O Decomposition over Zinc Cobaltite Catalysts

B. M. Abu-Zied*, S. A. Soliman, S. E. Abdellah

Chemistry Department, Faculty of Science, Assiut University, Assiut, Egypt
Email: *babuzied@aun.edu.eg

Abstract

In this paper, a series of zinc cobaltite catalysts with the general formula $Zn_xCo_{1-x}Co_2O_4$ (x = 0.25, 0.50, 0.75 and 1.0) has been prepared using the co-precipitation method. Thermal analyzes (TGA and DTA) were used to follow up the thermal events accompanying the heat treatment of the parent mixture. Based on these results, the various parent mixtures were calcined at 500°C. The obtained solid catalysts were characterized by using XRD, FT-IR and N_2-adsorption. The catalytic decomposition of N_2O to N_2 and O_2 was carried out on the zinc-cobaltite catalysts. It was found that partial replacement of Co^{2+} by Zn^{2+} in Co_3O_4 spinel oxide led to a significant improvement in their N_2O decomposition activity. Moreover, the catalytic activity was found to be depended on the calcination temperature utilized.

Keywords

Greenhouse Gases, Nitrous Oxide, N₂O Decomposition, $Zn_xCo_{1-x}Co_2O_4$, Zinc Cobaltite, Spinel Oxide

1. Introduction

In the last two decades, there has been considerable increased concern about the harmful effects of N_2O on our atmosphere. N_2O is recognized as a strong greenhouse gas and also severely destructs the ozone in the stratosphere [1] [2] [3] [4]. Moreover, it causes the formation of acid rains [4]. The atmospheric lifetime of nitrous oxide is about 120 years and its present concentration is 326 ppbv, whereas its Global Worming Potential (GWP) is 310 times higher than that of CO_2 [1]. The catalytic decomposition of N_2O to its elements, *i.e.* N_2 and O_2, is consi-

dered as an efficient rout to minimize its emission to the atmosphere.

Polycrystalline metal cobalt oxide (cobaltites) having the general formula MCo_2O_4 where M is divalent metal ion such as Mg, Mn, Zn, Ni, Co and Cu, have wide ranging applications in various technical fields [5]-[13]. It is established that various spinel cobaltites are effective catalysts for a number of industrial processes such as soot combustion [14], methane combustion [15] [16], methanol decomposition [17] [18] and the oxidation of various compounds such as cyclohexane [19], propane [20], CO [21] [22] and 2,3,5-trimethylphenol [23].

The catalytic decomposition of N_2O was investigated over various catalysts formulations. An interesting review on this topic was published recently by Konsolakis [3]. The reported state of the art catalytic systems is bare oxides, hexaaluminates, hydrotalcites, spinels, perovskites and mixed metal oxides under various effluent stream components (e.g., O_2, NO and H_2O) [3]. Among these catalysts categories, metal oxide based spinel catalysts revealed the lowest light off temperature (temperature corresponded to the 50% conversion). Therefore, focusing our attention to this catalysts category, high N_2O decomposition activity was exhibited by this class of catalysts [24]-[36]. For instance, Russo *et al.* [24] studied N_2O decomposition over a series of spinel oxide catalysts (chromites, ferrites and cobalties) being prepared by the solution combustion route. Their results indicated that the catalytic activity of the prepared spinel oxides essentially depended mostly on the B site metal (Cr, Fe and Co). The catalysts hosting cobalt at the B site presented the best N_2O decomposition activity [24]. Yan *et al.* [25] [26] reported an excellent catalytic performance of $M_xCo_{1-x}Co_2O_4$ (M = Mg^{2+}, Ni^{2+} and Zn^{2+}) spinel catalysts for the decomposition of nitrous oxide. The $Zn_{0.36}Co_{0.64}Co_2O_4$ catalyst is the most active in the studied samples. Highest activity performances were observed for $Mg_{0.54}Co_{0.46}Co_2O_4$, $Ni_{0.74}Co_{0.26}Co_2O_4$ and $Zn_{0.36}Co_{0.64}Co_2O_4$ compositions. It was shown that, Zr^{4+} doping (0.05 - 0.15 mol. %) of $ZnCo_2O_4$ led to the stabilization of this spinel at high calcination temperatures and improved its activity during N_2O decomposition [27]. Concurrently, Shen *et al.* [28] presented a detailed study on N_2O decomposition over different oxide supported Co_3O_4 spinel catalysts prepared via the co-precipitation method and found that Co_3O_4/MgO with cobalt loading of 15% showed the best activity, where a 100% conversion was obtained at temperatures higher than 425°C. The activity of the metal cobaltittes during N_2O decomposition is greatly enhanced by the presence of dopants. In this way, activity increase was reported on doping Co_3O_4 with Sr^{2+} and Ba^{2+} [29]. Concurrently, promotion effect was reported on doping $MgCo_2O_4$ with Li^+, Na^+, K^+ and Cs^+ [30].

Recently, we have reported the effect of transition metal exchange as well as the calcination temperature on the N_2O decomposition activity of $Ni_xCo_{1-x}Co_2O_4$ [31] and $Cu_xCo_{1-x}Co_2O_4$ [32] catalysts. Although the N_2O decomposition over zinc cobaltite catalysts was previously reported by Yan *et al.* [26], their catalysts were calcined at low temperature (400°C), which would not permit the activity measurement at higher temperatures. Therefore, and in a continuation of that work, our recent work [31] [32], the present paper attempts to prepare a series of $Zn_xCo_{1-x}Co_2O_4$ (x = 0.25, 0.50, 0.75 and 1.0) catalysts through the thermal

decomposition reactions of their corresponding metal carbonates at higher temperature (500°C). Our main goal is to study the oxygen evolution via N_2O decomposition over this series of catalysts. The catalysts were characterized using TGA, DTA, XRD, FT-IR and nitrogen adsorption at −196°C. Moreover, the experiments will be extended to check the influence of increasing the calcination temperature (up to 1000°C) on the activity of the best catalyst in this series.

2. Experimental

2.1. Catalysts Preparation

A series of catalysts with the general formula $Zn_xCo_{1-x}Co_2O_4$ (x = 0.0; 0.25; 0.50; 0.75 and 1.00) were synthesized by co-precipitation method [31] [32]. An aqueous solution of K_2CO_3 (1 M) was added drop-wise into a mixed aqueous solution containing known amounts of $Co(CH_3COO)_2 \cdot 4H_2O$ and $Zn(CH_3COO)_2 \cdot 4H_2O$ at room temperature under mechanical stirring until a pH value of 9.1 was reached. The precipitate was filtered, and then washed intensively with distilled water. Finally, the obtained cakes was dried overnight at 100°C and then calcined in static air at 500°C for 3 h. In order to investigate the influence of the calcination temperatures on the catalytic activity, two other catalysts (with x value = 0.75) were prepared employing the same procedure and calcined at 750 and 1000°C.

2.2. Catalytic Activity Measurements

The catalytic performances of the various $Zn_xCo_{1-x}Co_2O_4$ catalysts were evaluated in a quartz tube fixed-bed reactor. A mixture of the reactant N_2O (500 ppm) and the N_2 as a balance gas was fed at the constant rate of 200 ml·min^{-1} via two thermal mass flow controllers to the reactor, which is placed in an electric oven. For each experiment 0.5 g of the catalyst was used and pretreated in N_2 at 500°C for 1 h, then cooled to desired temperature. The temperature in the reactor was measured by a K-type thermocouple placed in the center of the catalyst bed and was controlled by a Cole-Parmer temperature controller (type Digi-Sense 89000-00). The inlet and outlet gases concentrations were analyzed with non-dispersive infrared analyzer for N_2O and NO components (ABB, AO2020-Uras 14) and amagnetic oxygen analyzer (ABB, AO2020-Magnos 106). All the experiments revealed the absence of NO in the reactor outlet gases.

2.3. Catalysts Characterization

Thermoanalytical measurements (TGA and DTA) were carried out using a Shimadzu DT-60 instrument apparatus. The sample (10 mg) was placed in a platinum crucible and heated at a heating rate of 10°C min^{-1} in air flowing at a rate of 40 ml·min^{-1}. XRD was used to check the formation of the spinel oxides structure in the prepared solids. X-ray diffraction patterns were obtained at room temperature using a Philips X-ray diffractometer (type PW 103/00) employing copper radiation (λ = 1.5405 Å). The X-ray tube was operated at 35 kV and 20 mA. The diffraction angle 2θ was scanned at a rate of 0.06 min^{-1}. The data were

analyzed using JCPDS standards cards. The FT-IR spectra were recorded at room temperature for the prepared catalysts in the wavelength region 4000 - 400 cm^{-1} using KBr disk technique. Nitrogen adsorption-desorption isotherms were constructed using a NOVA 3200e automated gas sorption system at liquid nitrogen temperature ($-196°C$). Prior to the measurements, each sample was degassed for 3 h at 250°C. The potassium ion concentrations in the various samples were determined by atomic adsorption using 210 VGP atomic absorption spectrophotometer.

3. Results and Discussion

3.1. Thermal Analyses

The thermal events accompanying the heat treatment, from ambient till 1000°C, of the non-calcined zinc/cobalt mixture, for the parent with x = 0.75, where monitored using TGA and DTA analyses. Inspection of the obtained TGA thermogram, **Figure 1(a)**, reveals the presence of four weight loss (WL) processes being maximized at 57, 246, 278 and 911°C. The first WL step describes the dehydration of the parent mixture. The second and the third WL steps are consecutive steps and could be attributed to the decomposition of both cobalt and zinc carbonates. In agreement with the reported work on $Cu_{0.75}Co_{0.25}Co_2O_4$ [32], $Ni_{0.75}Co_{0.25}Co_2O_4$ [31] and bare Co_3O_4 [37] [38] [39] [40] [41], the final WL could be assigned to the decomposition of the spinel oxide. The relevant DTA thermogram (**Figure 1(b)**) manifests that the dehydration process is characterized by a broad endothermic effect at 65°C. The exothermic effect observed at 225°C can be related to the decomposition of cobalt carbonate together with the $Co^{2+} \rightarrow Co^{3+}$ transformation [37] [38] [39] [40] [41]. One could suggest that, the observed broad endothermic effect at 250°C - 315°C together with the exothermic one at 276°C are due to the supper-position of zinc carbonate decomposition and zinc cobaltite formation, respectively. Such suggestion is reinforced by the following points: 1) the observed similar phenomena in case of Ni/Co and Cu/Co mixture [31] [32]; and 2) the reported exothermic effect accompanying the
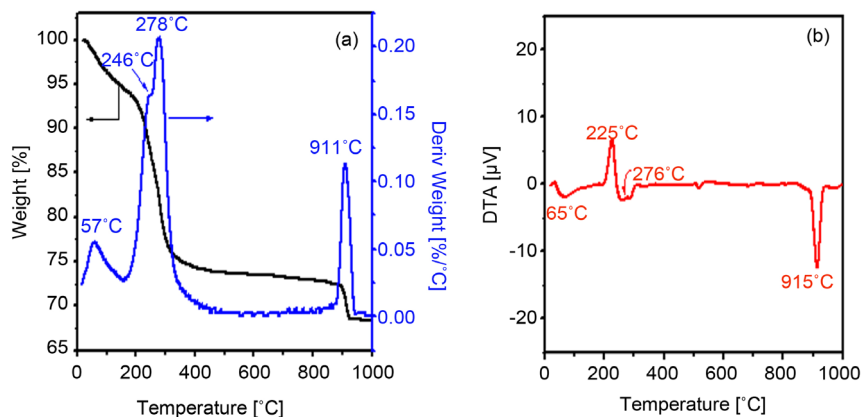
Figure 1. TGA (a) and DTA (b) thermograms obtained for zinc/cobalt mixture with x = 0.75.

$ZnCo_2O_4$ formation, using other precursors, at the same temperature range [42] [43]. Finally, as reported for other similar systems [31] [32] [37] [38] [39] [40] [41], the observed endothermic peak at 915°C could be attribute to the decomposition of $ZnCo_2O_4$ spinel yielding a mixture of its constituent oxides.

3.2. X-Ray Diffraction

X-ray diffraction patterns were determined for the 500°C calcination products of the Zn/Co mixtures. The obtained patterns (Figure 2) were matched with the authentic JCPDS data in order to characterize the phases formed during the calcination process. Our analysis showed that the obtained difractogrames matched well with those standards of Co_3O_4 (JCPDS 78-1969) and $ZnCo_2O_4$ (JCPDS 81-2299), which are reported by many research groups [27] [42] [43] [44] [45] [46]. In addition, weak intensity reflections attributable to ZnO (JCPDS 80-0075) were also found with increasing the x-value. In this respect, it was demonstrated that heating zinc cabaltite at temperatures as such as 500°C leads to its partial decomposition forming ZnO [27] [43]. Moreover, doping $ZnCo_2O_4$ with oxides like ZrO_2 enhances its thermal stability at 550°C - 750°C temperature range [27]. The catalysts crystallite sizes were calculated using Scherrer equation. The obtained values for the zinc-containing catalysts (Table 1) are lower than that of the bare Co_3O_4 (28 nm) [31]. The estimated potassium ion concentrations are, also, listed in Table 1. All the zinc-containing spinels exhibit higher potassium content compared to the bare spinel (0.18 mg·g^{-1}) [31].

Since the $Zn_{0.75}Co_{0.25}Co_2O_4$ catalyst exhibited the best performance during
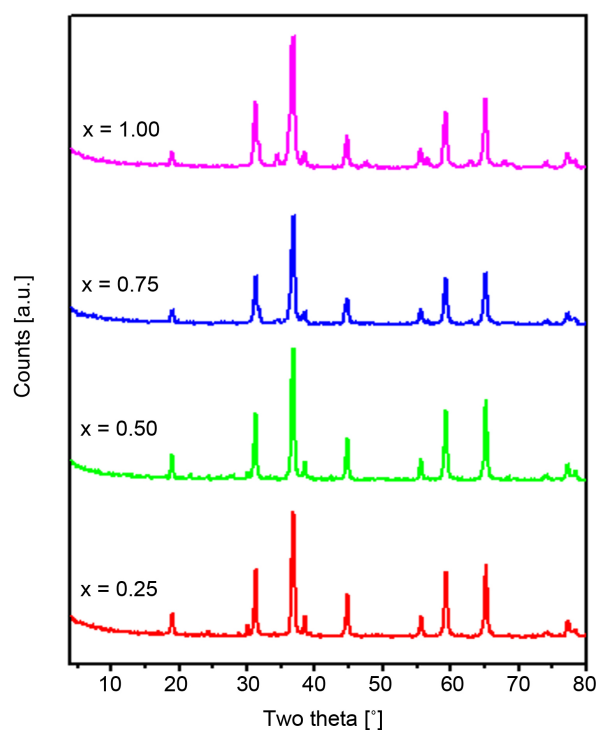
Figure 2. XRD powder diffractograms obtained for the Zn-Co catalysts calcined at 500°C.

Table 1. Crystallites size and K^+ concentrations in the various Zn-Co mixtures calcined at 500°C.

Catalyst	Crystallite size [nm]	Residual potassium [mg·g^{-1}]
$Zn_{0.25}Co_{0.75}Co_2O_4$	24	14
$Zn_{0.50}Co_{0.50}Co_2O_4$	23	15
$Zn_{0.75}Co_{0.25}Co_2O_4$	20	4.2
$ZnCo_2O_4$	21	3.4

N_2O decomposition (*vide infra*), the study was extended to check the effect of increasing the calcination temperature on its activity. **Figure 3** shows the XRD patterns for the Zn/Co mixture with x = 0.75, which are calcined at 500°C, 750°C and 1000°C. It is evident that raising the calcination temperature from 500°C to 750°C leads to: 1) a marked decrease in the intensity of the reflections due to ZnO; and 2) an intensity increase of all the peaks due to the spinel oxide. Further increase in the calcinations temperature to 1000°C resulted in a dramatic change in the obtained XRD pattern. One can spot the fact that the intensity of all reflections showed marked decrease. In addition, new reflections emerged at: 1) 2θ = 36.72°, 42.32° and 61.42° attributable to CoO (JCPDS 75-0533); and 2) at 2θ = 31.75°, 34.44°, 47.57°, 56.62°, 62.91° and 69.09° characterizing ZnO (JCPDS 80-0075). This picture suggests that zinc cobaltite decomposes to the oxides of its constituents, *i.e.*, zinc and cobalt oxide. This goes paralleled with the observed WL at 911°C in the relevant TG thermogram (**Figure 1(a)**).

3.3. FT-IR Spectra

Figure 4 depicts the FTIR spectra of $Zn_xCo_{1-x}Co_2O_4$ (x = 0.25, 0.50, 0.75 and 1.00) catalysts being calcined for 3 h in air at 500°C. All the obtained spectra manifest the presence of two absorption bands in the region 663 - 669 and 564 - 573 cm^{-1} corresponding to metal-oxygen stretching from tetrahedral and octahedral sites, respectively, which are characteristic for metal cobaltites [23] [27] [30] [37] [38] [39] [40] [41]. Moreover, the obtained spectra for the various catalysts illustrate the presence of weak absorptions at 836 - 848 and 1110 - 1116 cm^{-1} and broad strong ones at 1443 - 1455 cm^{-1}. Such absorptions are due to the carbonate anions [27] [47]. In this regard, the detection of the carbonate absorptions for these samples goes parallel with the measured residual potassium ions concentration for the zinc containing catalysts (**Table 1**). The spectra of the two catalysts having x = 0.75 and 1.00 show a weak absorption at 480 cm^{-1}, which is characteristic of the ZnO phase [43] [48]. This in turn, suggests the presence of ZnO as an impurity for these two catalysts. Such finding agrees well with the information gathered from the XRD analysis in the previous section. All the spectra show two other bands at 1642 and 3200 - 3600 cm^{-1}, which are due to the δ (OH) and ν (O-H) modes of water molecules, respectively [27] [31] [32].

Figure 5 shows the FT-IR spectra of the catalyst with x-value of 0.75 being calcined at the 500°C - 1000°C temperature range. Inspection of this Figure
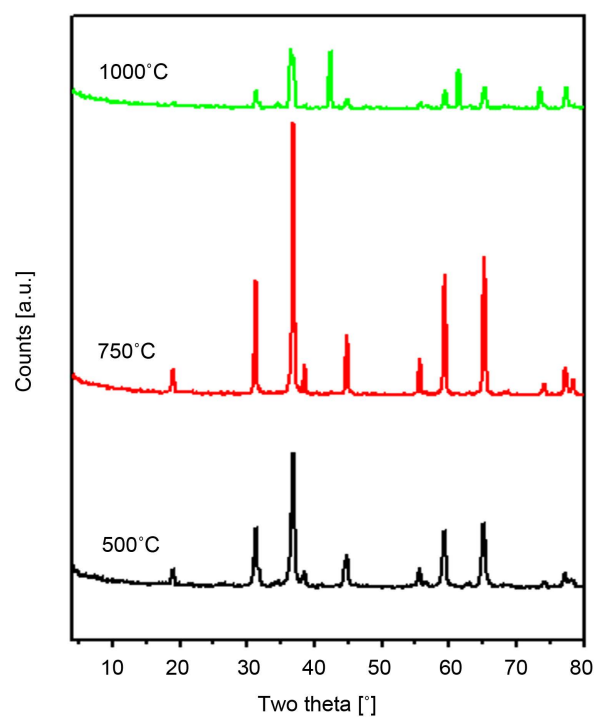
Figure 3. X-ray powder diffractograms obtained for $Zn_{0.75}Co_{0.25}Co_2O_4$ catalysts being prepared by the co-precipitation method and calcined at 500°C, 750°C and 1000°C.
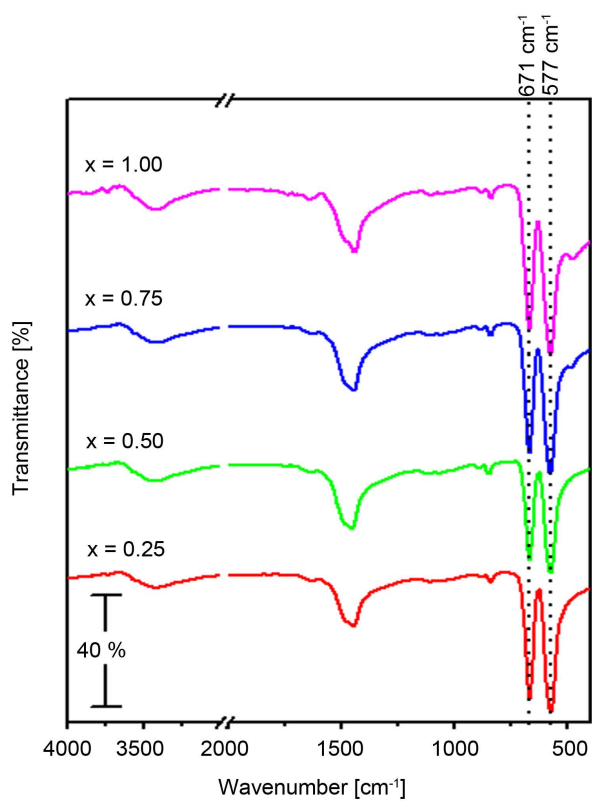
Figure 4. FT-IR spectra obtained for $Zn_xCo_{1-x}Co_2O_4$ (x = 0.25, 0.50, 0.75 and 1.00) being prepared by the co-precipitation method and calcined at 500°C.
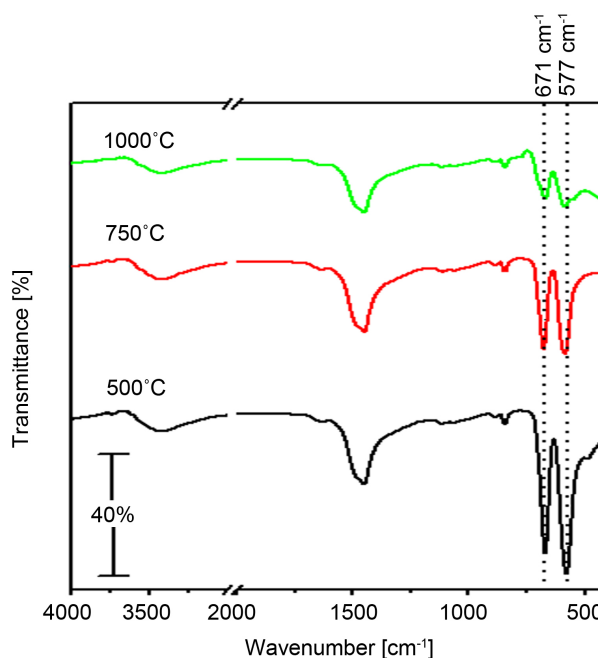
Figure 5. FT-IR spectra obtained for $Zn_{0.75}Co_{0.25}Co_2O_4$ being prepared by the co-precipitation method and calcined at 500˚C, 750˚C and 1000˚C.

reveals that all spectra show the two bands characterizing the Zn-Co spinel structure at 577 and 671 cm^{-1}. However, the intensity of these two absorptions decreases continuously with the calcination temperature rise. Concurrently, Kostova *et al.* [48] reported that the intensity of the Zn-Co spinel bands, v_1 and v_2, increase with temperature increasing to as high as 700˚C. The intensities of these bands stop to increase at 800˚C and decrease after treatment at 900˚C. Such result is in a good agreement with the XRD analysis for the same samples [48]. All the obtained spectra (**Figure 5**) indicate the persistence of the absorptions due to the carbonate phase with the temperature raise. For the sample calcined at 750˚C, one can notice the disappearance of the absorption due to ZnO at 480 cm^{-1}, which suggests the presence of zinc as Zn-Co spinel only without ZnO impurities. Such suggestion is in a good agreement with the XRD results (**Figure 3**). The spectrum for the 1000˚C calcined catalyst shows a weak absorption at 553 which is due to the CoO [49] [50].

3.4. N$_2$ Adsorption

N$_2$ adsorption data of the catalyst with x = 0.0 is published elsewhere [32]. Nitrogen adsorption-desorption isotherm s of the zinc-containing catalysts being calcined at 500˚C are plotted in **Figure 6**. As it can be seen from that Figure the introduction of Zn to the Co$_3$O$_4$ with x = 0.25 and 0.50 leads to the increase in the Type I character of the obtained isotherms. Further increase in the Zn content till x = 1.00 is accompanied by recovering of isotherms Type II character. The specific surface areas of these adsorbents were calculated using the BET equation and the obtained values are tabulated in **Table 2**. It is obvious that S$_{BET}$
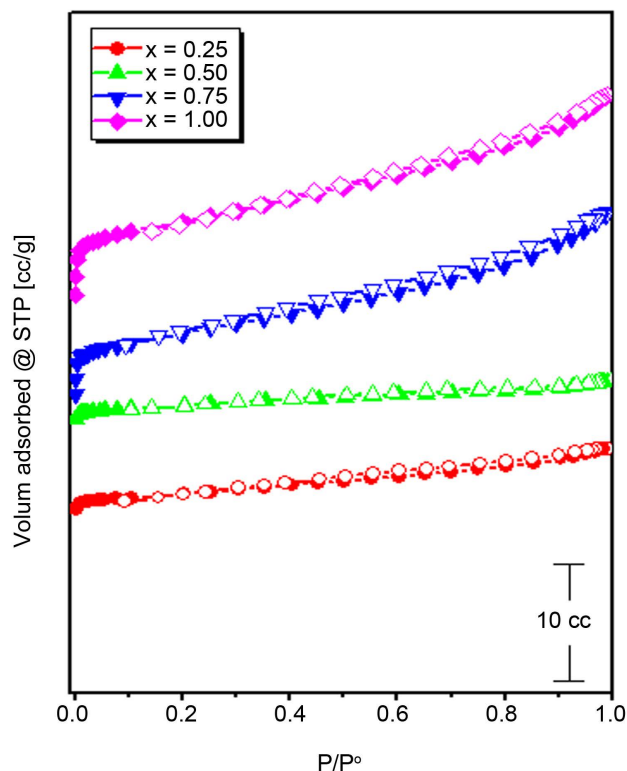
Figure 6. Nitrogen adsorption-desorption isotherms of the $Zn_xCo_{1-x}Co_2O_4$ catalysts calcined at 500˚C (closed symbols refer to adsorption branches whereas open ones refer to desorption branches).

decreases as the x-value increases till x = 0.50 followed by an increase on further x-value increase till x = 1.00. **Figure 7(a)** depicts the V_{a-t} graphs for the $Zn_xCo_{1-x}Co_2O_4$ catalysts. $Zn_{0.50}Co_{0.50}Co_2O_4$ catalyst shows only a downward deviation indicating its micro-porosity. The rest of the samples in this series exhibit an upward followed by downward deviations, indicating the dual nature, *i.e.* micro- and meso-porosity, of these adsorbents. The external surface areas, S_t, micropore surface areas and micropore volumes were computed from volume-thickness curves, V_{a-t} plots of various investigated adsorbents in this series and are listed in **Table 2**. An inspection of the data given in **Table 2** reveals that the trend of variation of these parameters with x-value is similar to that shown for the S_{BET} variation. The pore size distribution curves for the different adsorbents in the Zn/Co catalysts prepared by the co-precipitation method and calcined at 500˚C are shown in **Figure 7(b)**. One can easily spot the fact that all the samples, with the exception of $Zn_{0.50}Co_{0.50}Co_2O_4$, show a broad peak maximized at 21 - 25 Å. Such peaks lie at the meso-porous and at the vicinity of the micro-porous one. Such finding goes parallel with the information abstracted from the V_{a-t} plots (**Figure 7(a)**).

Nitrogen adsorption-desorption isotherms of the $Zn_{0.75}Co_{0.25}Co_2O_4$ catalyst being calcined at 750˚C and 1000˚C (not shown) indicate that raising the calcination temperature from 500˚C to 1000˚C is accompanied by a gradual
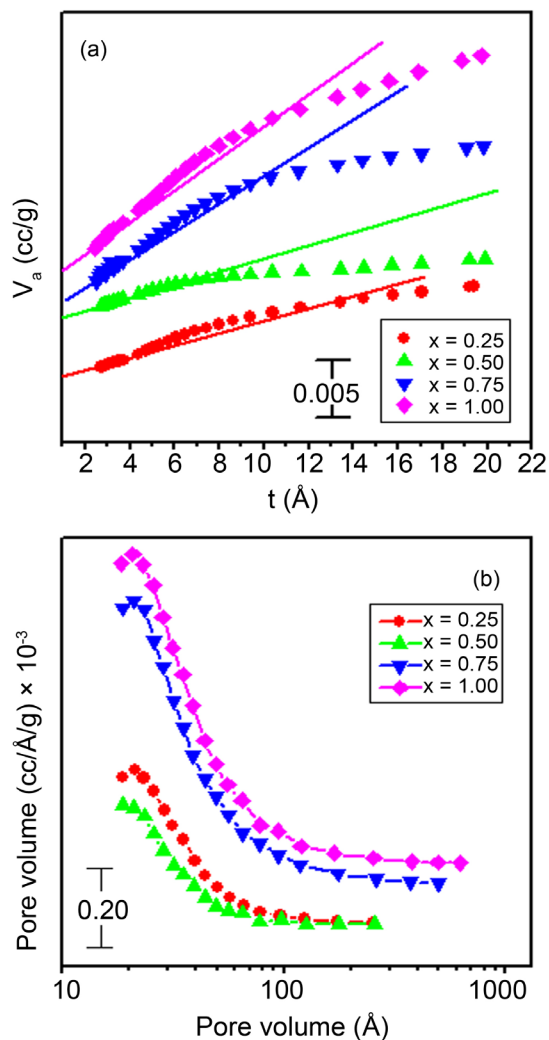
Figure 7. $V_{a\text{-}t}$ plots (a) and Pore volume distribution curves (b) obtained for the $Zn_xCo_{1-x}Co_2O_4$ catalysts calcined at 500°C.

Table 2. Texture data obtained from the analysis of nitrogen sorption isotherms of the $Zn_xCo_{1-x}Co_2O_4$ catalysts being calcined at 500°C.

X-value	S_{BET} [m²/g]	External surface area [m²/g]	Micropore surface area [m²/g]	Total pore volume [10^{-2} cc/g]	Micropore volume [10^{-3} cc/g]	Average pore diameter [Å]
0.25	8.32	7.51	0.81	0.948	0.472	45.85
0.50	6.55	5.85	0.70	0.589	0.314	35.97
0.75	20.82	18.73	2.09	2.474	1.047	47.52
1.00	25.64	21.71	3.92	2.765	1.992	43.14
$Zn_{0.75}$-750°C	11.86	9.19	2.67	1.288	1.358	43.47
$Zn_{0.75}$-1000°C	2.25	1.69	0.56	0.268	0.000	47.49

transformation of Type II to Type I of the obtained isotherms. Following the variation of S_{BET} values with the calcination temperature they obtained values,

Table 2, manifests that, as expected, raising the calcination temperature to 1000°C is accompanied by a continuous S_{BET} and S_t decrease. Moreover, Table 2 indicates that this decrease is accompanied by a continuous decrease in both the micropore and the total pore volumes.

3.5. N$_2$O Decomposition Activity

Figure 8(a) shows the variation of N$_2$O conversion with x-value over $Zn_xCo_{1-x}Co_2O_4$ catalysts at 150°C - 500°C temperature range. Inspection of this Figure reveals that all over the reactor temperature range increasing the zinc ions content, *i.e.*, x-value, leads to a continuous activity increase till x = 0.75. Further increase in the Zn^{2+} concentration, *i.e.*, for the $ZnCo_2O_4$ catalyst, results in a slight activity decrease. The relevant T_{50} values of these catalysts together with that of the catalyst with x = 0.00 [31] [32] are shown in Figure 8(b). From the inspection of Figure 8(b), it appears that all the Zn-containing catalysts exhibit higher activity than Co_3O_4, x = 0.00, *i.e.*, lower T_{50} values, where the lowest value is exhibited by the catalyst with x = 0.75. This finding agrees well with the reported results for bare Co_3O_4 measured under the same experimental conditions [31] [32]. The dependence of the activity promotion on the Zn-concentration was also reported for this system of catalysts by Yan *et al.* [25]. Their results
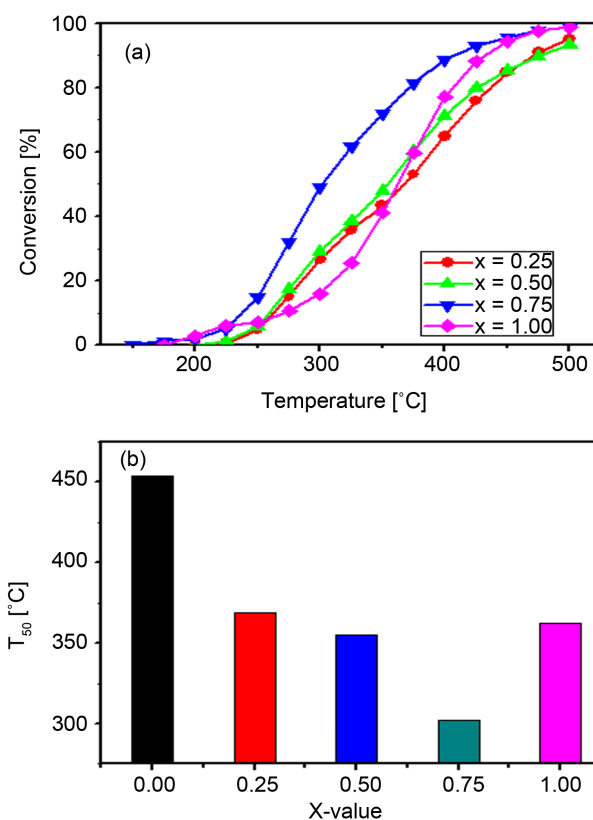
Figure 8. Variation of the N$_2$O conversion percentage on the reactor temperature (a) and the variation of T_{50}-value with the x-value (b) for the various $Zn_xCo_{1-x}Co_2O_4$ catalysts calcined at 500°C.

showed that the partial replacement of Co^{2+} by Zn^{2+} in Co_3O_4 spinel oxide led to a significant improvement in the catalytic activity for the N_2O decomposition, and the $Zn_{0.36}Co_{0.64}Co_2O_4$ catalyst was the most active in their investigated samples. However, the precise origins of the observed high activities have not been reported in their studies. This observed difference in catalytic activity for N_2O decomposition, between the data presented in Figure 8 and the report of Yan *et al.* [25], could be due to the difference of preparation method and post-synthesis treatment of the precursor compounds.

The obtained high activity of the Zn/Co catalysts compared to the bare Co_3O_4 spinel oxide catalyst [31] [32] can be understood in terms of the following points: 1) From the catalysts characterization data, it was shown that the thermal reduction of the spinel phase to its components, for the catalyst with x = 0.75, occurs at 915°C as shown by the endothermic peak in Figure 1(b). In comparison to the bare Co_3O_4, which decomposes at 930°C [34], it appears that the addition of zinc ions enhances the reduction of Co^{3+} ions. This, again, supports the promotional role of the added transition metal cation (Zn^{2+}) during N_2O decomposition throughout facilitating the redox cycle $Co^{2+} \rightarrow Co^{3+} \rightarrow Co^{2+}$ and thus increasing the catalytic activity [29] [30] [31] [32]. 2) The calculated crystallite sizes of the various catalysts (Table 1). In comparison with the crystallite size of pure Co_3O_4 catalyst, 28 nm [31], it is evident that the values of all Zn^{2+} containing catalysts are lower than that of pure Co_3O_4 catalyst. Moreover, the trend of variation in these values with x-values is similar to that observed during N_2O decomposition over this series of catalysts. Therefore, it is plausible to suggest that, the observed activity patterns of this series of catalysts are also influenced by the spinel crystallite size. This finding is in a good agreement with the reported N_2O decomposition increases upon decreasing catalysts crystallite size of $Mg_xCo_{1-x}Co_2O_4$ [29], $Ni_xCo_{1-x}Co_2O_4$ [31], $Cu_xCo_{1-x}Co_2O_4$ [32], $Ag/Fe_xAl_{2-x}O_3$ [51] and $SrCO_3$- and $BaCO_3$-Co_3O_4 [30] catalysts. 3) The high activity of the zinc containing catalysts can be attributed, again, to their higher potassium ions content, compared to the Co_3O_4 [31], and the higher S_{BET} values for the catalysts having x = 0.75 and 1.00.

The reported mechanism for N_2O decomposition over cobalt oxide spinel catalysts requires the presence of Co^{2+}-Co^{3+} surface-redox couples [29] [30] according to:

$$N_2O_{(g)} + Co^{2+} \rightarrow N_2O^-_{(ads.)} \cdots Co^{3+}. \tag{1}$$

$$N_2O^-_{(ads.)} \cdots Co^{3+} \rightarrow N_{2(g)} + O^-_{(ads.)} \cdots Co^{3+}. \tag{2}$$

$$O^-_{(ads.)} \cdots Co^{3+} \rightarrow 1/2 O_{2(g)} + Co^{2+}. \tag{3}$$
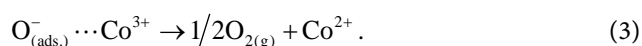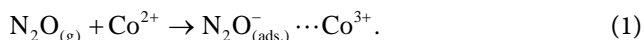
In this mechanism, the regeneration of the catalysts active centers, *i.e.*, Co^{2+} is crucial for maintaining the catalytic activity. The higher activity of $MgCo_2O_4$ compared to bare Co_3O_4 for N_2O decomposition was correlated with shift of the high temperature endothermic peak, ascribed to $Co^{3+} \rightarrow Co^{2+}$ towards lower temperatures [29]. Figure 9 shows the DTA thermogram of bare Co_3O_4 and $Ni_{0.75}Co_{0.25}Co_2O_4$ catalysts. One can easily detect the presence on an endothermic
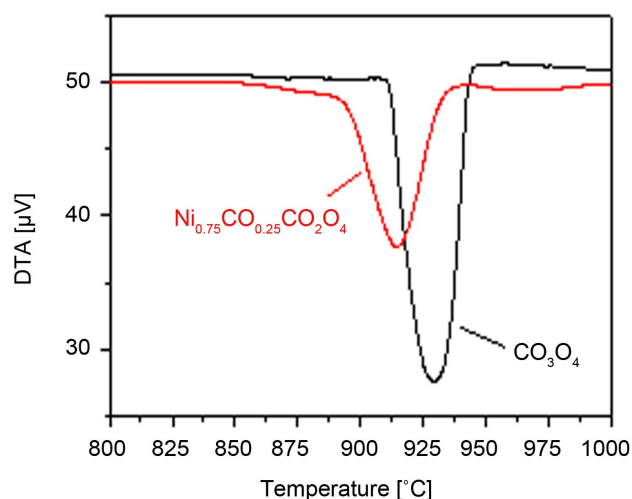
Figure 9. DTA thermograms of bare Co_3O_4 and $Zn_{0.75}Co_{0.25}Co_2O_4$ catalysts.

effect at 930°C for bare Co_3O_4., which could attributed to the $Co^{3+} \rightarrow Co^{2+}$ thermal reduction [37] [38] [39] [40]. The presence of nickel ions, *i.e.*, for $Ni_{0.75}Co_{0.25}Co_2O_4$ catalyst shifts this peak to 915°C. In other words, the presence of nickel ions enhances the thermal reduction of Co^{3+} facilitating the regeneration of Co^{2+} active sites. Accordingly, the same role of nickel ions could be suggested under catalytic conditions, *i.e.*, the presence of these ions, together with potassium ions [29] [31] [32], enhances the recoverability of the catalysts active centers (Co^{2+}) as shown by equation No. 3. Concurrently and based on the DTA temperature shift, Wilczkowska *et al*. [36] reported an enhancement effect of oxygen presence in the reactor feed during N_2O decomposition over Co_3O_4 at 850°C. Such effect was correlated with the role of oxygen in reforming Co_3O_4 via its reaction with CoO, which is formed via the thermal reduction of Co_3O_4 at high temperatures. Xue *et al*. [35] pointed out the importance of surface area increase in enhancing the N_2O decomposition over ceria promoted Co_3O_4 catalysts. Similar findings were reported for Mg/Co catalysts [29]. Therefore, the higher surface areas of the catalysts with X = 0.75 and 1.00, especially at high reactor temperatures, offer more active centers participating in N_2O adsorption and thus increasing the activity.

In the previous paragraphs, it was shown that $Zn_{0.75}Co_{0.25}Co_2O_4$ catalyst shows the best performance during N_2O decomposition. To our knowledge, in the open literature there is a lack of information about the influence of increasing the calcination temperature on the N_2O abetment activity of Zn/Co catalysts. Therefore, in a similar to that followed in Ni/Co and Cu/Co catalysts, the catalyst with x = 0.75 was calcined at 750°C and 1000°C. **Figure 10** shows the dependence of of N_2O conversion percentage on the reactor temperature over $Zn_{0.75}Co_{0.25}Co_2O_4$ catalyst being calcined at 500°, 750°C and 1000°C. The data presented in **Figure 10** manifests that raising the calcination temperature from 500°C to 750°C leads to a noticeable activity decrease. In this regard, the T_{50} value shows about 100°C shift to higher temperatures as a result of such pretreatment temperature
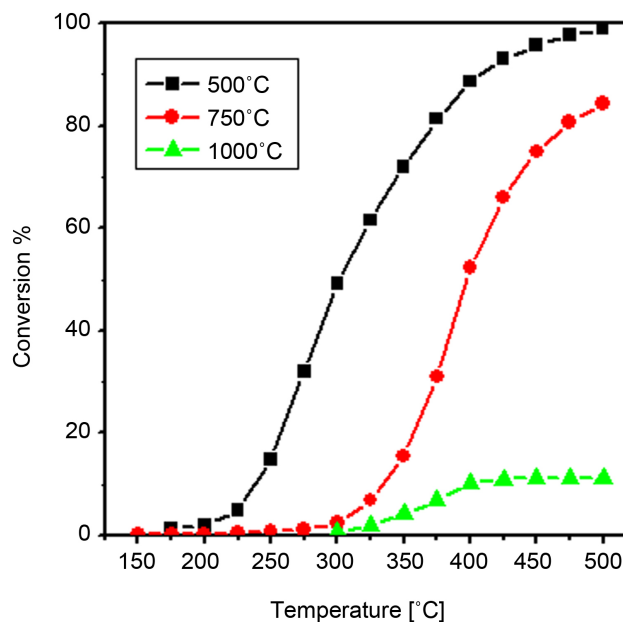
Figure 10. Dependence of N_2O conversion percentage on the reaction temperature over $Zn_{0.75}Co_{0.25}Co_2O_4$ catalyst being calcined at 500˚C, 750˚C and 1000˚C.

rise. Pushing the calcination temperature to 1000˚C is accompanied by a sharp drop in the activity where the maximum conversion did not exceed 12% at 500˚C reactor temperature.

The characterization results demonstrated that calcining this composition at 750˚C leads to the formation of the perfect spinel structure. Therefore, it is plausible to relate the observed activity decrease to the observed decrease in the BET surface area (Table 2) as well as the expected crystallite size increase at such temperature. Regarding the 1000˚C calcined catalyst, it was also concluded from the characterization data that at such pretreatment temperature zinc cobaltite decomposes to the oxides of its constituents, *i.e.*, zinc and cobalt oxide, together with the $Co^{3+} \rightarrow Co^{2+}$ reduction. Thus, one can state safely that in addition to the sintering effects which predominate at high temperatures, the observed sharp activity decrease for the 1000˚C calcined catalyst is influenced by the structure modifications taking place at such high temperature. Such modifications would lead to a retardation of the $Co^{2+} \rightarrow Co^{3+} \rightarrow Co^{2+}$ redox cycle which is essential for N_2O decomposition [29] [30] [31] [32].

4. Conclusion

This paper focuses on the preparation and activity evaluation of zinc substituted Co_3O_4 catalysts, $Zn_xCo_{1-x}Co_2O_4$ (x = 0.25, 0.50, 0.75 and 1.0) through the thermal decomposition reactions of their corresponding metal carbonates. Characterization techniques indicated that the prepared catalysts adopt the spinel structure, which decomposed at high temperatures (930˚C). These catalysts were tested for N_2O-direct decomposition at 150˚C - 500˚C reactor temperatures. The obtained results indicate that these catalysts are promising candidates for low temperature

N$_2$O abatement. The N$_2$O conversion activity is influenced by various parameters which include the nickel content, the crystallite size, the residual potassium ions, catalyst surface area and the calcination temperature. The optimum balance of these parameters, which leads to the highest activity, is fulfilled by the 500˚C calcined Zn$_{0.75}$Co$_{0.25}$Co$_2$O$_4$ catalyst.

Acknowledgements

References

[1] Pérez-Ramírez, J. (2007) Prospects of N$_2$O Emission Regulations in the European Fertilizer Industry. *Applied Catalysis B: Environmental*, **70**, 31-35.
https://doi.org/10.1016/j.apcatb.2005.11.019

[2] Pérez-Ramírez, J., Kapteijn, F., Schöffel, K. and Moulijn, J.A. (2003) Formation and Control of N$_2$O in Nitric Acid Production: Where Do We Stand Today? *Applied Catalysis B: Environmental*, **44**, 117-151.
https://doi.org/10.1016/S0926-3373(03)00026-2

[3] Konsolakis, M. (2015) Recent Advances on Nitrous Oxide (N$_2$O) Decomposition over Non-Noble-Metal Oxide Catalysts: Catalytic Performance, Mechanistic Considerations, and Surface Chemistry Aspects. *ACS Catalysis*, **5**, 6397-6421.
https://doi.org/10.1021/acscatal.5b01605

[4] Abu-Zied, B.M. and Schwieger, W. (2009) Self Oscillatory Behaviour in N$_2$O Decomposition over Co-ZSM-5 Catalysts. *Applied Catalysis B: Environmental*, **85**, 120-130. https://doi.org/10.1016/j.apcatb.2008.07.002

[5] Shan, Y. and Gao, L. (2007) Formation and Characterization of Multi-Walled Carbon Nanotubes/Co$_3$O$_4$ Nanocomposites for Supercapacitors. *Materials Chemistry and Physics*, **103**, 206-210. https://doi.org/10.1016/j.matchemphys.2007.02.038

[6] Kanazawa, E., Sakai, G., Shimanoe, K., Kanmura, Y., Teraoka, Y., Miura, N. and Yamazoe, N. (2001) Metal Oxide Semiconductor N$_2$O Sensor for Medical Use. *Sensors and Actuators B: Chemical*, **77**, 72-77.
https://doi.org/10.1016/S0925-4005(01)00675-X

[7] Sharma, Y., Sharma, N., Rao, G.V.S. and Chowdari, B.V.R. (2008) Studies on Spinel Cobaltites, FeCo$_2$O$_4$ and MgCo$_2$O$_4$ as Anodes for Li-Ion Batteries. *Solid State Ionics*, **179**, 587-597. https://doi.org/10.1016/j.ssi.2008.04.007

[8] Sharma, Y., Sharma, N., Rao, G.V.S. and Chowdari, B.V.R. (2007) Nanophase ZnCo$_2$O$_4$ as a High Performance Anode Material for Li-Ion Batteries. *Advanced Functional Materials*, **17**, 2855-2861. https://doi.org/10.1002/adfm.200600997

[9] Sharma, Y., Sharma, N., Rao, G.V.S. and Chowdari, B.V.R. (2007) Lithium Recycling Behaviour of Nano-Phase-CuCo$_2$O$_4$ as Anode for Lithium-Ion Batteries. *Journal of Power Sources*, **173**, 495-501. https://doi.org/10.1016/j.jpowsour.2007.06.022

[10] Liu, Y., Mi, C.H., Su, L. and Zhang, X. (2008) Hydrothermal Synthesis of Co$_3$O$_4$ Microspheres as Anode Material for Lithium-Ion Batteries. *Electrochimica Acta*, **53**, 2507-2513. https://doi.org/10.1016/j.electacta.2007.10.020

[11] Lichtenberg, F. and Kleinsorgen, K. (1996) Stability Enhancement of the CoOOH Conductive Network of Nickel Hydroxide Electrodes. *Journal of Power Sources*, **62**, 207-211. https://doi.org/10.1016/S0378-7753(96)02431-7

[12] Makhlouf, S.A. (2002) Magnetic Properties of Co_3O_4 Nanoparticles. *Journal of Magnetism and Magnetic Materials*, **246**, 184-190. https://doi.org/10.1016/S0304-8853(02)00050-1

[13] Yamaura, H., Moriya, K., Miura, N. and Yamazoe, N. (2000) Mechanism of Sensitivity Promotion in CO Sensor Using Indium Oxide and Cobalt Oxide. *Sensors and Actuators B*, **65**, 39-41. https://doi.org/10.1016/S0925-4005(99)00456-6

[14] Liu, J., Zhao, Z., Wang, J., Xu, C., Duan, A., Jiang, G. and Yang, Q. (2008) The Highly Active Catalysts of Nanometric CeO_2-Supported Cobalt Oxides for Soot Combustion. *Applied Catalysis B: Environmental*, **84**, 185-195. https://doi.org/10.1016/j.apcatb.2008.03.017

[15] Ulla, M.A., Spretz, R., Lombardo, E., Daniell, W. and Knözinger, H. (2000) Catalytic Combustion of Methane on Co/MgO: Characterisation of Active Cobalt Sites. *Applied Catalysis B: Environmental*, **29**, 217-229. https://doi.org/10.1016/S0926-3373(00)00204-6

[16] Xiao, T.-C., Fuji, S., Wang, H.-T., Coleman, K.S. and Green, M.L.H. (2001) Methane Combustion over Supported Cobalt Catalysts. *Journal of Molecular Catalysis A: Chemical*, **175**, 111-123. https://doi.org/10.1016/S1381-1169(01)00205-9

[17] Manova, E., Tsoncheva, T., Paneva, D., Mitov, I., Tenchev, K. and Petrov, L. (2004) Mechanochemically Synthesized Nano-Dimensional Iron-Cobalt Spinel Oxides as Catalysts for Methanol Decomposition. *Applied Catalysis A: General*, **277**, 119-127. https://doi.org/10.1016/j.apcata.2004.09.002

[18] Manova, E., Tsoncheva, T., Estournès, Cl., Paneva, D., Tenchev, K., Mitov, I. and Petrov, L. (2006) Nanosized Iron and Iron-Cobalt Spinel Oxides as Catalysts for Methanol Decomposition. *Applied Catalysis A: General*, **300**, 170-180. https://doi.org/10.1016/j.apcata.2005.11.005

[19] Zhou, L., Xu, J., Miao, H., Wang, F. and Li, X. (2005) Catalytic Oxidation of Cyclohexane to Cyclohexanol and Cyclohexanone over Co_3O_4 Nanocrystals with Molecular Oxygen. *Applied Catalysis A: General*, **292**, 223-228. https://doi.org/10.1016/j.apcata.2005.06.018

[20] Liu, Q., Wang, L.-C., Chen, M., Cao, Y., He, H.-Y. and Fan, K.-N. (2009) Dry Citrate-Precursor Synthesized Nanocrystalline Cobalt Oxide as Highly Active Catalyst for Total Oxidation of Propane. *Journal of Catalysis*, **263**, 104-113. https://doi.org/10.1016/j.jcat.2009.01.018

[21] Wang, Y.-Z., Zhao, Y.-X., Gao, C.-G. and Liu., D.-S. (2007) Preparation and Catalytic Performance of Co_3O_4 Catalysts for Low-Temperature CO Oxidation. *Catalysis Letters*, **116**, 136-142. https://doi.org/10.1007/s10562-007-9099-4

[22] Lin, H.K., Chiu, H.C., Tsai, H.C., Chien, S.H. and Wang, C.B. (2003) Synthesis, Characterization and Catalytic Oxidation of Carbon Monoxide over Cobalt Oxide. *Catalysis Letters*, **88**, 169-174. https://doi.org/10.1023/A:1024013822986

[23] Li, Y., Liu, W., Wu, M., Yi, Z. and Zhang, J. (2007) Oxidation of 2,3,5-Trimethylphenol to 2,3,5-Trimethylbenzoquinone with Aqueous Hydrogen Peroxide in the Presence of Spinel $CuCo_2O_4$. *Journal of Molecular Catalysis A: Chemical*, **261**, 73-78. https://doi.org/10.1016/j.molcata.2006.07.067

[24] Russo, N., Fino, D., Saracco, G. and Specchia, V. (2007) N_2O Catalytic Decomposition over Various Spinel-Type Oxides. *Catalysis Today*, **119**, 228-232. https://doi.org/10.1016/j.cattod.2006.08.012

[25] Yan, L., Ren, T., Wang, X., Gao, Q., Ji, D. and Suo, J. (2003) Excellent Catalytic Performance of $Zn_xCo_{1-x}Co_2O_4$ Spinel Catalysts for the Decomposition of Nitrous Oxide. *Catalysis Communications*, **4**, 505-509. https://doi.org/10.1016/S1566-7367(03)00131-6

[26] Yan, L., Ren, T., Wang, X., Ji, D. and Suo, J. (2003) Catalytic Decomposition of N_2O over $M_xCo_{1-x}Co_2O_4$ (M = Ni, Mg) Spinel Oxides. *Applied Catalysis B: Environmental*, **45**, 85-90. https://doi.org/10.1016/S0926-3373(03)00174-7

[27] Basahel, S.N., Abd El-Maksod, I.H., Abu-Zied, B.M. and Mokhtar, M. (2010) Effect of Zr^{4+} Doping on the Stabilization of ZnCo-Mixed Oxide Spinel System and Its Catalytic Activity towards N_2O Decomposition, *Journal of Alloys and Compounds*. **493**, 630-635. https://doi.org/10.1016/j.jallcom.2009.12.169

[28] Shen, Q., Li, L., Li, J., Tian, H. and Hao, Z. (2009) A Study on N_2O Catalytic Decomposition over Co/MgO Catalysts. *Journal of Hazardous Materials*, **163**, 1332-1337. https://doi.org/10.1016/j.jhazmat.2008.07.104

[29] Abu-Zied, B.M. (2011) Nitrous Oxide Decomposition over Alkali-Promoted Magnesium Cobaltite Catalysts. *Chinese Journal of Catalysis*, **32**, 264-272. https://doi.org/10.1016/S1872-2067(10)60174-X

[30] Abu-Zied, B.M. and Soliman, S.A. (2009) Nitrous Oxide Decomposition over MCO_3-Co_3O_4 (M = Ca, Sr, Ba) Catalysts. *Catalysis Letters*, **132**, 299-310. https://doi.org/10.1007/s10562-009-0158-x

[31] Abu-Zied, B.M., Soliman, S.A. and Abdellah, S.E. (2014) Pure and Ni-Substituted Co_3O_4 Spinel Catalysts for Direct N_2O Decomposition. *Chinese Journal of Catalysis*, **35**, 1105-1112. https://doi.org/10.1016/S1872-2067(14)60058-9

[32] Abu-Zied, B.M., Soliman, S.A. and Abdellah, S.E. (2015) Enhanced Direct N_2O Decomposition Over $Cu_xCo_{1-x}Co_2O_4$ (0.0 ≤ x ≤ 1.0) Spinel-Oxide Catalysts. *Journal of Industrial and Engineering Chemistry*, **21**, 814-821. https://doi.org/10.1016/j.jiec.2014.04.017

[33] Obalová, L., Jirátová, K., Kovanda, F., Pacultová, K., Lacný, Z. and Mikulova, Z. (2005) Catalytic Decomposition of Nitrous Oxide over Catalysts Prepared from Co/Mg-Mn/Al Hydrotalcite-Like Compounds. *Applied Catalysis B: Environmental*, **60**, 289-297. https://doi.org/10.1016/j.apcatb.2005.04.002

[34] Karásková, K., Obalová, L. and Kovanda, F. (2011) N_2O Catalytic Decomposition and Temperature Programmed Desorption Tests on Alkali Metals Promoted Co-Mn-Al Mixed Oxide. *Catalysis Today*, **176**, 208-211. https://doi.org/10.1016/j.cattod.2010.12.055

[35] Xue, L., Zhang, C., He, H. and Teraoka, Y. (2007) Catalytic Decomposition of N_2O over CeO_2 Promoted Co_3O_4 Spinel Catalyst. *Applied Catalysis B: Environmental*, **75**, 167-174. https://doi.org/10.1016/j.apcatb.2007.04.013

[36] Wilczkowska, E., Krawczyk, K., Petryk, J., Sobczak, J.W. and Kaszkur, Z. (2010) Direct Nitrous Oxide Decomposition with a Cobalt Oxide Catalyst. *Applied Catalysis A: General*, **389**,165-172. https://doi.org/10.1016/j.apcata.2010.09.016

[37] Makhlouf, M.T., Abu-Zied, B.M. and Mansoure, T.H. (2013) Effect of Calcination Temperature on the H_2O_2 Decomposition Activity of Nano-Crystalline Co_3O_4 Prepared by Combustion Method. *Applied Surface Science*, **274**, 45-52. https://doi.org/10.1016/j.apsusc.2013.02.075

[38] Makhlouf, M.T., Abu-Zied, B.M. and Mansoure, T.H. (2014) Effect of Fuel/Oxidizer Ratio and the Calcination Temperature on the Preparation of Microporous-Nanostructured Tricobalt Tetraoxide. *Advanced Powder Technology*, **25**, 560-566. https://doi.org/10.1016/j.apt.2013.09.003

[39] Makhlouf, M.T., Abu-Zied, B.M. and Mansoure, T.H. (2013) Nanocrystalline Co_3O_4 Fabricated via the Combustion Method. *Metals and Materials International*, **19**, 489-495. https://doi.org/10.1007/s12540-013-3017-7

[40] Makhlouf, M.T., Abu-Zied, B.M. and Mansoure, T.H. (2013) Direct Fabrication of Cobalt Oxide Nanoparticles Employing Sucrose as a Combustion Fuel. *Journal of*

Nanoparticles, **2013**, Article ID: 384350. https://doi.org/10.1155/2013/384350

[41] Makhlouf, M.T., Abu-Zied, B.M. and Mansoure, T.H. (2012) Direct Fabrication of Cobalt Oxide Nano-Particles Employing Glycine as a Combustion Fuel. *Physical Chemistry*, **2**, 86-93. https://doi.org/10.5923/j.pc.20120206.01

[42] Wei, X., Chen, D. and Tang, W. (2007) Preparation and Characterization of the Spinel Oxide $ZnCo_2O_4$ Obtained by Sol-Gel Method. *Materials Chemistry and Physics*, **103**, 54-58. https://doi.org/10.1016/j.matchemphys.2007.01.006

[43] Song, F., Huang, L., Chen, D. and Tang, W. (2008) Preparation and Characterization of Nanosized Zn-Co Spinel Oxide by Solid State Reaction Method. *Materials Letters*, **62**, 543-547. https://doi.org/10.1016/j.matlet.2007.06.015

[44] Zhang, G.Y., Guo, B. and Chen, J. (2006) MCo_2O_4 (M = Ni, Cu, Zn) Nanotubes: Template Synthesis and Application in Gas Sensors. *Sensors and Actuators B*, **114**, 402-409. https://doi.org/10.1016/j.snb.2005.06.010

[45] Niu, X., Du, W. and Du, W. (2004) Preparation and Gas Sensing Properties of ZnM_2O_4 (M = Fe, Co, Cr). *Sensors and Actuators B*, **99**, 405-409. https://doi.org/10.1016/j.snb.2003.12.007

[46] Kim, H.J., Song, I.C., Sim, J.H., Kim, H., Kim, D., Ihm, Y.E. and Choo, W.K. (2004) Structural and Transport Properties of Cubic Spinel $ZnCo_2O_4$ Thin Films Grown by Reactive Magnetron Sputtering. *Solid State Communications*, **129**, 627-630. https://doi.org/10.1016/j.ssc.2003.12.025

[47] Lefez, B., Nkeng, P., Lopitaux, J. and Poillerat, G. (1996) Characterization of Cobaltite Spinels by Reflectance Spectroscopy. *Materials Research Bulletin*, **31**, 1263-1267. https://doi.org/10.1016/0025-5408(96)00122-5

[48] Kustova, G.N., Burgina, E.B., Volkova, G.G., Yurieva, T.M. and Plyasova, L.M. (2000) IR Spectroscopic Investigation of Cation Distribution in Zn-Co Oxide Catalysts with Spinel Type Structure. *Journal of Molecular Catalysis A*: *Chemical*, **158**, 293-296. https://doi.org/10.1016/S1381-1169(00)00093-5

[49] Guo, Q., Guo, X. and Tian, Q. (2010) Optionally Ultra-Fast Synthesis of CoO/Co_3O_4 Particles Using $CoCl_2$ Solution via a Versatile Spray Roasting Method. *Advanced Powder Technology*, **21**, 529-533. https://doi.org/10.1016/j.apt.2010.02.003

[50] Tang, C.-W., Wang, C.-B. and Chien, S.-H. (2008) Characterization of Cobalt Oxides Studied by FT-IR, Raman, TPR and TG-MS. *Thermochimica Acta*, **473**, 68-73. https://doi.org/10.1016/j.tca.2008.04.015

[51] Abu-Zied, B.M. (2008) Oxygen Evolution over $Ag/Fe_xAl_{2-x}O_3$ ($0.0 \leq x \leq 2.0$) Catalysts via N_2O and H_2O_2 Decomposition. *Applied Catalysis A*: *General*, **334**, 234-242. https://doi.org/10.1016/j.apcata.2007.10.013